PERGAMON

International Journal of Solids and Structures 39 (2002) 2587–2612

INTERNATIONAL JOURNAL OF SOLIDS and STRUCTURES

www.elsevier.com/locate/ijsolstr

Micromechanical analysis of the fully coupled finite thermoelastic response of rubber-like matrix composites

Jacob Aboudi *

Faculty of Engineering, Tel-Aviv University, Ramat-Aviv 69978, Israel

Received 22 January 2001; received in revised form 21 January 2002

Abstract

A micromechanical analysis for the prediction of the coupled thermoelastic response of multiphase composites that include rubber-like phases is presented. Rubber-like solids are highly nonlinear thermoelastic materials that exhibit anomalous behavior referred to as the thermoelastic inversion effect. Results are presented which show that the derived micromechanical model is capable of predicting this effect in nylon/rubber composites subjected to appropriate thermal loadings assuming one-way coupling. For full thermomechanical coupling, the nonlinear response and induced temperatures under several types of mechanical loading are investigated.

Keywords: Rubber-like solids; Finite thermoelasticity; Thermoelastic inversion effect; Multiphase materials; Micromechanics; Homogenization

1. Introduction

Operating at temperatures above their glass transition zone, rubber-like materials, of which vulcanized natural rubber is the prototype, have the ability to sustain large thermoelastic deformations, but return to their original shape when the loading is removed. Vulcanized rubber is formed by combining natural rubber with sulfur, and its glass transition temperature is approximately 213 K (Treloar, 1975). Rubber-like materials exhibit a distinctive characteristic referred to as the thermoelastic inversion effect. In ordinary materials (e.g. metals and ceramics) that are subjected to prescribed extensions, the gradient of stress with respect to temperature is always negative. In rubber-like material on the other hand, this gradient becomes positive at prescribed extensions beyond a critical level, thereafter increasing with extension. Similarly, in ordinary materials that are subjected to prescribed loadings, the gradient of deformation with respect to temperature is always positive. In rubber-like materials this gradient becomes negative for loadings beyond a critical value, thereafter decreasing with loading. Thus, beyond this critical value the rubber has a negative coefficient of thermal expansion. This anomalous behavior of rubber-like solids can be demonstrated

* Fax: +972-3-640-7617.
E-mail address: aboudi@eng.tau.ac.il (J. Aboudi).

0020-7683/02/$ - see front matter
PII: S0020-7683(02)00126-9

by hanging a weight on a strip of rubber and changing the temperature. The weight will rise upwards when the rubber is heated and it will lower when it is cooled.

Free energy functions that are capable of representing the large thermoelastic deformation of rubber-like materials including the thermoelastic inversion effect have been offered by Chadwick (1974), Chadwick and Creasy (1984), Ogden (1992) and Morman (1995), for example. A discussion of the thermodynamics of rubber-like solids has been given by Price (1976).

When the rubber-like material is combined with other materials such as nylon fibers or steel wires, a rubber-like matrix composite is obtained. Tires form an example of layered multiphase flexible composite structures that consist of rubbery matrices and stiff reinforcements made of steel wires or synthetic fibers. The high modulus, low elongation cords carry most of the load, and the low modulus, high elongation rubber matrix preserves the integrity of the composite and transfers the load. The primary objective of this type of composite is to withstand large deformation and fatigue loading while providing high load carrying capacity.

A micromechanical model that is capable of predicting the finite thermoelastic behavior of multiphase composites in which one or more phases are rubber-like materials has been presented by Aboudi (2001a). The behavior of the rubber-like matrix was described by the Helmholtz free energy function that was developed by Chadwick (1974), Chadwick and Creasy (1984), and Morman (1995). This free energy formulation models the large thermoelastic deformation of the unreinforced matrix material, and is able to capture the thermoelastic inversion effect. Aboudi (2001a) demonstrated that the micromechanical analysis was capable of quantitatively predicting the finite deformation and the thermoelastic inversion effect of the rubber-like matrix composites subjected to various types of loading (hydrostatic loading, thermal loading with prescribed extension, thermal loading with prescribed stress, free thermal expansion, and isothermal uniaxial loading). This micromechanical analysis was carried out assuming a one-way coupling, namely, under the assumption that the temperature field is not coupled to the mechanical deformation. Thus, as in thermal stress problems, the temperature field was prescribed independently. It is, however, more realistic to consider the effect of coupling that exists between the finite mechanical deformation and the temperature field in rubber-like matrix composites. This is the subject of the present investigation. To this end, the coupled energy equation is incorporated into the micromechanical analysis. Consequently, the global mechanical response and the induced temperature field that result from an applied macroscopic mechanical loading can now be predicted.

In the present paper a micromechanical multiphase model is offered for the analysis of the coupled large thermoelastic deformation of rubber-like matrix composites. This analysis is based on the homogenization theory, according to which the field is assumed to vary on multiple spatial scales due to the existence of a microstructure. It is also assumed that the microstructure is spatially periodic, and that the field variables can be approximated by an asymptotic expansion. The resulting governing equations in the homogenization method are typically solved numerically, using the finite element approach. For a literature review and implementation of this method in the framework of small deformation, we mention Suquet (1987), Jansson (1992) and Banks-Sills et al. (1997) where a host of references to investigators using the homogenization approach are given. For papers in which the homogenization procedure is employed to examine the large mechanical deformations of composite materials, see Agah-Tehrani (1990) and Takano et al. (2000), for example.

The homogenization theory that is employed in this paper establishes the strong form of the differential equations that govern the first two terms of the asymptotic expansion of the displacement variables. To this end, the fully coupled large thermoelastic constitutive equations, in conjunction with the equilibrium and energy equations that govern the behavior of the constituents, are employed in order to establish the response of the composite that is subjected to an external mechanical field. The resulting governing differential equations are solved analytically by an approximate method using concepts that were previously employed in constructing a higher-order theory for functionally graded materials (Aboudi et al., 1999). In

the special case of linearly elastic phases with thermal stresses, the present approach reduces to that which has been previously presented by Aboudi et al. (2001).

The derived micromechanical analysis, which is based on the tangent approach in conjunction with an incremental procedure, can predict the overall behavior of nonlinearly thermoelastic multiphase composites. Every constituent in such a composite can be assumed, in general, to behave as a thermoelastic rubber-like material with finite deformation. As a result of the tangent approach, it is necessary to solve at each time increment a system of linear algebraic equations. Furthermore, in the course of the micromechanical analysis, the instantaneous thermomechanical concentration tensors (which relate the local deformation gradient and temperature to the global applied deformation gradient), are established. In addition, the effective current tangent tensor (which relates the average stress increment to the average deformation gradient increment), is established. Both the concentration and tangent tensors are given at each time increment in a closed-form manner in terms of the geometrical dimensions and material properties of the phases.

In addition to steel wires, synthetic cords such as nylon, polyester, and ryon are often employed to reinforce rubbery matrices. Herein, application of the derived micromechanical analysis are given for nylon/rubber-like matrix composites. We start with the uncoupled thermomechanical theory to demonstrate the occurrence of the thermoelastic inversion effect in the composite when it is subjected to thermal loading with prescribed extensions and thermal loading with prescribed stresses. The thermoelastic inversion effect in the composite is well exhibited in these cases. Next, the fully coupled theory is employed to study the thermomechanical response and the induced temperature in a composite that is subjected to hydrostatic, axial, transverse and biaxial transverse loading. In Appendix A the constitutive law of a rubber-like material and the associated energy equation are established.

2. Homogenization

Consider a multiphase composite in which the microstructures are distributed periodically in the three-dimensional space that is given in terms of the global initial coordinates (X_1, X_2, X_3), which describe the location of the particle at time $t = 0$ in the undeformed configuration, see Fig. 1(a) and (b) which shows the repeating unit cell of the periodic composite. In the framework of the homogenization method, the displacement rates $\dot{u}_i$ are asymptotically expanded in terms of a small parameter as follows:

$$\dot{u}_i(\mathbf{X}) = \dot{u}_{0i}(\mathbf{X}, \mathbf{Y}) + \delta \dot{u}_{1i}(\mathbf{X}, \mathbf{Y}) + \cdots \quad i = 1\text{–}3 \tag{1}$$

where $\mathbf{X} = (X_1, X_2, X_3)$ are the initial macroscopic (global) coordinate system, and $\mathbf{Y} = (Y_1, Y_2, Y_3)$ are the microscopic (local) initial coordinates that are defined with respect to the repeating unit cell. The size of the unit cell is further assumed to be much smaller than the size of the body so that the relation between the global and local systems is

$$Y_i = \frac{X_i}{\delta} \tag{2}$$

where δ is a small scaling parameter characterizing the size of the unit cell. This implies that a movement of order unity on the local scale corresponds to a very small movement on the global scale.

The homogenization method is applied to composites with periodic microstructures. Thus

$$\dot{u}_{\alpha i}(\mathbf{X}, \mathbf{Y}) = \dot{u}_{\alpha i}(\mathbf{X}, \mathbf{Y} + n_p \mathbf{d}_p) \tag{3}$$

with $\alpha = 0, 1, \ldots$, where n_p are arbitrary integer numbers and the constant vectors $\mathbf{d}_p$ determine the period of the structure.

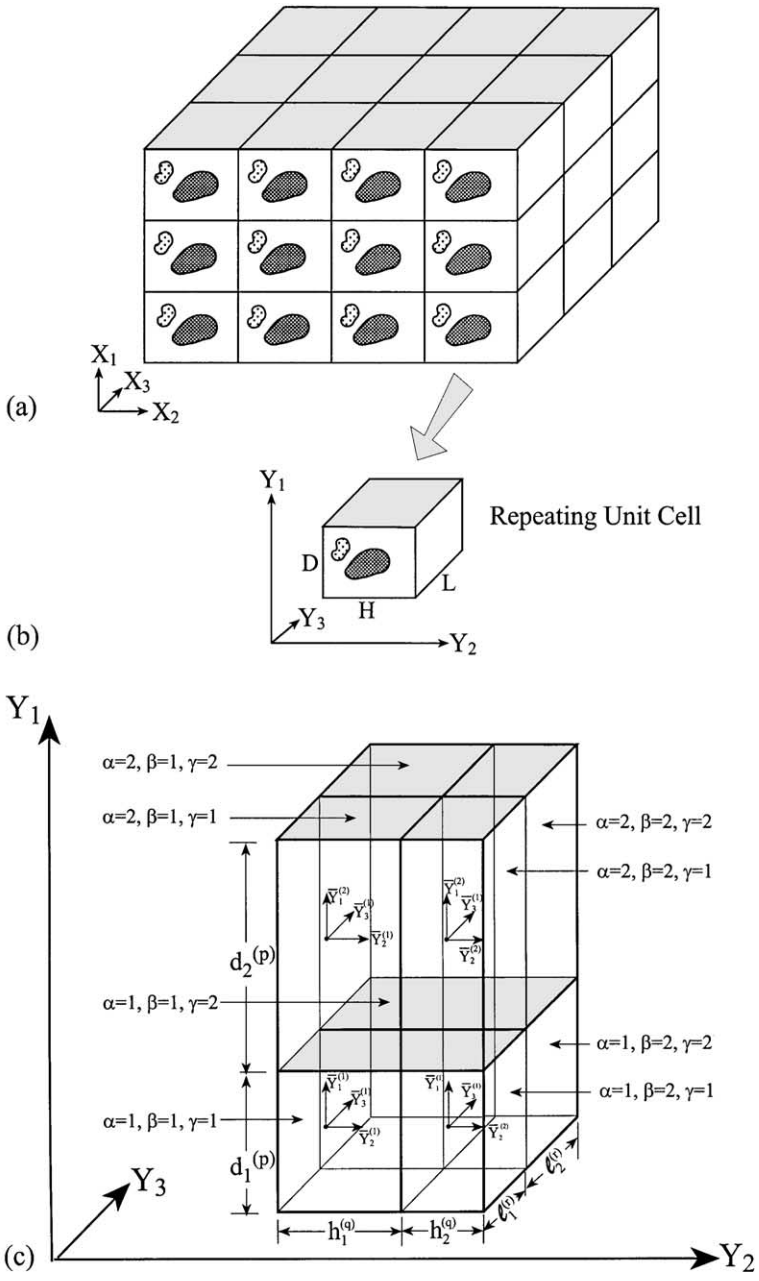

Fig. 1. (a) A multiphase composite with periodic microstructure, (b) the repeating unit cell and (c) a typical generic cell (labeled as (p,q,r)) into several of which the repeating unit cell is discretized. The generic cell consists of eight subcells.

Due to the change of coordinates from the global to the local systems the following relation must be employed in evaluating the derivative of a field quantity:

$$\frac{\partial}{\partial X_i} \to \frac{\partial}{\partial X_i} + \frac{1}{\delta}\frac{\partial}{\partial Y_i} \tag{4}$$

The quantities $\dot{u}_{0i}$ are the rate of displacements in the homogenized region and hence they are not functions of Y_i.

Let

$$\dot{u}_{0i} = \dot{u}_{0i}(\mathbf{X}) \equiv \dot{\bar{u}}_i \tag{5}$$

and

$$\dot{u}_{1i} \equiv \dot{\tilde{u}}_i(\mathbf{X}, \mathbf{Y}) \tag{6}$$

where the latter are the fluctuating displacement rates, which are unknown periodic functions with respect to $\mathbf{Y}$. These displacement rates arise due to the heterogeneity of the medium.

The rates of the displacement gradient components are determined from the displacement expansion rates (1) yielding, in conjunction with Eq. (4), the following expression

$$\dot{F}_{ij} = \dot{\overline{F}}_{ij}(\mathbf{X}) + \dot{\widetilde{F}}_{ij}(\mathbf{X}, \mathbf{Y}) + O(\delta) \quad i, j = 1\text{–}3 \tag{7}$$

where

$$\overline{F}_{ij}(\mathbf{X}) = \frac{\partial \bar{u}_i}{\partial X_j} \tag{8}$$

and

$$\widetilde{F}_{ij}(\mathbf{X}, \mathbf{Y}) = \frac{\partial \tilde{u}_i}{\partial Y_j} \tag{9}$$

This shows that the rates of the displacement gradient components can be represented as a sum of the displacement gradient rates $\overline{F}_{ij}(\mathbf{X})$ in the composite and fluctuating displacement gradient rates $\widetilde{F}_{ij}(\mathbf{X}, \mathbf{Y})$.

The average of the displacement gradient rates in the repeating unit cell is determined from

$$\frac{1}{V_Y}\int_{V_Y} \dot{F}_{ij}\,\mathrm{d}V_Y = \frac{1}{V_Y}\int_{V_Y} (\dot{\overline{F}}_{ij} + \dot{\widetilde{F}}_{ij})\,\mathrm{d}V_Y = \dot{\overline{F}}_{ij} + \frac{1}{V_Y}\int_{\Gamma_Y} \dot{\tilde{u}}_i N_j\,\mathrm{d}\Gamma_Y = \dot{\overline{F}}_{ij} \tag{10}$$

where the divergence theorem has been employed with V_Y being the volume of the repeating unit cell and Γ_Y is its surface. The resulting surface integral is zero because the fluctuating displacement rates $\dot{\tilde{u}}_i$, being periodic, are equal on the opposite sides of the unit cell, while the normal N_j has opposite directions. For a homogeneous material it is obvious that the fluctuating displacements and displacement gradients identically vanish.

For a composite that is subjected to homogeneous deformation, one can use of Eq. (7) to represent the displacement rates in the form

$$\dot{u}_i(\mathbf{X}, \mathbf{Y}) = \dot{\overline{F}}_{ij} X_j + \dot{\tilde{u}}_i + O(\delta^2) \tag{11}$$

The tangential form of the constitutive law of finite deformable thermoelastic materials has been established in Eq. (A.34). In the repeating unit cell region this constitutive law takes the form

$$\dot{\mathbf{T}} = \mathbf{R}(\mathbf{Y})\dot{\mathbf{F}} - \mathbf{H}(\mathbf{Y})\dot{\theta} \tag{12}$$

where $\mathbf{T}$ is the first Piola–Kirchhoff stress tensor, $\mathbf{R}$ is the fourth order instantaneous mechanical tangent tensor, $\mathbf{H}$ is the instantaneous thermal tangent second order tensor, and θ is the temperature field in the unit cell.

The form of the Lagrangian equilibrium equations in the repeating unit cell are given, in the absence of body forces, by (Malvern, 1969):

$$\frac{\partial \dot{T}_{ij}}{\partial Y_i} = 0 \tag{13}$$

In order to establish the equilibrium equations in the framework of the present homogenization procedure, let us substitute (7) into (12) and differentiate the result with respect to the microvariable coordinates Y_i of the repeating unit cell. This yields

$$\frac{\partial}{\partial Y_i}\left\{R_{ijkl}(\mathbf{Y})[\dot{\bar{F}}_{kl}(\mathbf{X}) + \dot{\tilde{F}}_{kl}(\mathbf{X},\mathbf{Y})] - H_{ij}(\mathbf{Y})\dot{\theta}(\mathbf{Y})\right\} = 0 \tag{14}$$

Let us define

$$\dot{T}^0_{ij} = R_{ijkl}(\mathbf{Y})\dot{\bar{F}}_{kl}(\mathbf{X}) \tag{15}$$

and

$$\dot{\tilde{T}}_{ij} = R_{ijkl}(\mathbf{Y})\dot{\tilde{F}}_{kl}(\mathbf{X},\mathbf{Y}) - H_{ij}(\mathbf{Y})\dot{\theta}(\mathbf{Y}) \tag{16}$$

with the latter being the fluctuating stresses.

The use of these definitions in Eq. (14) implies that

$$\frac{\partial \dot{\tilde{T}}_{ij}}{\partial Y_i} + \frac{\partial \dot{T}^0_{ij}}{\partial Y_i} = 0 \tag{17}$$

Eq. (17) is the strong form of the Lagrangian equilibrium equations of the homogenization theory. It is readily seen that the first terms in (17) involve the unknown fluctuating periodic displacement rates $\dot{\tilde{u}}_i$ while the second terms in these equations produce pseudo-body forces. It should be noted that, since the dependence of T^0_{ij} on $\mathbf{Y}$ is due to the term $R_{ijkl}(\mathbf{Y})$ (see Eq. (15)), the derivatives $\partial \dot{T}^0_{ij}/\partial Y_i$ (i.e., the pseudo-body forces) are zero within any phase of the repeating unit cell except at the boundaries between two different phases (where different values of the tangent tensors exist) at which it becomes nonzero.

For imposed values of the average deformation gradient rates $\dot{\bar{F}}_{kl}$ the unknown fluctuating displacements and the associated induced local temperature are governed by Eq. (17) and the coupled heat equation (A.25) subject to periodic boundary conditions that are prescribed at the boundaries of the repeating unit cell.

Referring to Fig. 1(b), the periodic boundary conditions are expressed by the requirement that the displacement, traction, temperature and heat flux should be equal on opposite sides of the repeating unit cell. Thus at the top and bottom surfaces, right and left surfaces, and front and rear surfaces of the repeating unit cell the displacement, traction, temperature and heat flux should be identical

$$\begin{aligned} \tilde{u}_i|_{\text{bottom}} &= \tilde{u}_i|_{\text{top}} \\ T_{1j}|_{\text{bottom}} &= T_{1j}|_{\text{top}} \\ \theta|_{\text{bottom}} &= \theta|_{\text{top}} \\ q_1|_{\text{bottom}} &= q_1|_{\text{top}} \end{aligned} \tag{18}$$

$$\begin{aligned} \tilde{u}_i|_{\text{left}} &= \tilde{u}_i|_{\text{right}} \\ T_{2j}|_{\text{left}} &= T_{2j}|_{\text{right}} \\ \theta|_{\text{left}} &= \theta|_{\text{right}} \\ q_2|_{\text{left}} &= q_2|_{\text{right}} \end{aligned} \tag{19}$$

$$\begin{aligned}
\tilde{\boldsymbol{u}}_i|_{\text{front}} &= \tilde{\boldsymbol{u}}_i|_{\text{rear}} \\
T_{3j}|_{\text{front}} &= T_{3j}|_{\text{rear}} \\
\theta|_{\text{front}} &= \theta|_{\text{rear}} \\
q_3|_{\text{front}} &= q_3|_{\text{rear}}
\end{aligned} \tag{20}$$

where T_{ij} $(i,j = 1\text{–}3)$ denotes the total Piola–Kirchhoff stress components given by

$$T_{ij} = T_{ij}^0 + \tilde{T}_{ij} \tag{21}$$

and q_i is the heat flux (see Eq. (A.27)).

In addition to these periodic boundary conditions one needs to impose continuity of displacement, traction, temperature and heat flux at the internal interfaces between the phases that fill the repeating unit cell.

3. The concentration tensors

Once the solution of Eq. (17) and the associated coupled heat equation (A.25), subject to the internal interfacial conditions and periodic boundary conditions (18)–(20) has been established, one can proceed and determine the concentration tensors associated with the defined repeating unit cell. These tensors express the local rate of deformation gradient and the induced rate of temperature in the cell in terms of the rate of the global applied external deformation gradient (localization). As will be shown in the next section, the determination of these tensors establishes the instantaneous effective stiffness tensor of the composite, which relates the rate of the average stress in the composite to the rate of applied displacement gradient (i.e., it provides the current requested global behavior of the multiphase composite, or, in other words, the overall tangential constitutive law).

To this end let us define the mechanical concentration tensor $\widetilde{\mathbf{A}}$ as follows:

$$\dot{\tilde{\mathbf{F}}} = \widetilde{\mathbf{A}}(\mathbf{Y})\dot{\overline{\mathbf{F}}} \tag{22}$$

It relates the rate of the fluctuating deformation gradient $\dot{\tilde{\boldsymbol{F}}}$ to the rate of applied global deformation gradient $\dot{\overline{\mathbf{F}}}$. Similarly, we define the thermal concentration tensor $\mathbf{a}$ as

$$\dot{\theta} = \mathbf{a}(\mathbf{Y})\dot{\overline{\mathbf{F}}} \tag{23}$$

which relates the induced local rate of temperature to $\dot{\overline{\mathbf{F}}}$. By using Eq. (7), we readily obtain the requested concentration tensor $\mathbf{A}(\mathbf{Y})$ as follows:

$$\dot{\mathbf{F}} = \dot{\overline{\mathbf{F}}} + \widetilde{\mathbf{A}}(\mathbf{Y})\dot{\overline{\mathbf{F}}} = [\mathbf{I}_4 + \widetilde{\mathbf{A}}(\mathbf{Y})]\dot{\overline{\mathbf{F}}} \equiv \mathbf{A}(\mathbf{Y})\dot{\overline{\mathbf{F}}} \tag{24}$$

where $\mathbf{I}_4$ is the fourth order identity tensor.

To obtain the concentration tensors $\mathbf{A}(\mathbf{Y})$ and $\mathbf{a}(\mathbf{Y})$ a series of problems must be solved as follows: solve Eq. (17) and the associated coupled heat equation (A.25) in conjunction with the internal interfacial and periodic boundary conditions with $\overline{F}_{11} = 1$ and all other components of $\overline{\mathbf{F}}$ being equal to zero. The solution of these coupled differential equations readily provides A_{ij11} for $i,j = 1\text{–}3$ and a_{11}. This procedure is repeated with $\overline{F}_{22} = 1$ and all other components of $\overline{\mathbf{F}}$ equal to zero which provides A_{ij22}, and a_{22}, etc.

4. The instantaneous effective stiffness tensor

Once the current concentration tensors $\mathbf{A}(\mathbf{Y})$ and $\mathbf{a}(\mathbf{Y})$ have been determined, it is possible to compute the effective stiffness tensor $\mathbf{R}^*$ of the multiphase composite as follows: substitution of $\dot{\mathbf{F}}$ and $\dot{\theta}$ given by (24) and (23), respectively, in Eq. (12) yields

$$\dot{\mathbf{T}} = [\mathbf{R}(\mathbf{Y})\mathbf{A}(\mathbf{Y}) - \mathbf{H}(\mathbf{Y})\mathbf{a}(\mathbf{Y})]\dot{\overline{\mathbf{F}}} \tag{25}$$

Taking the average of both sides of Eq. (25) over the repeating unit cell yields the rate of average stress in the composite in terms of the rate of average deformation gradient via the effective stiffness tensor $\mathbf{R}^*$, namely

$$\dot{\overline{\mathbf{T}}} = \mathbf{R}^*\dot{\overline{\mathbf{F}}} \tag{26}$$

where

$$\mathbf{R}^* = \frac{1}{V_Y}\int [\mathbf{R}(\mathbf{Y})\mathbf{A}(\mathbf{Y}) - \mathbf{H}(\mathbf{Y})\mathbf{a}(\mathbf{Y})]\,\mathrm{d}V_Y \tag{27}$$

It should be noted that the established instantaneous effective stiffness tensor involves the induced thermal effects due to the local coupling between mechanical and thermal fields.

5. Method of solution

In this section we present a solution methodology for Eqs. (17) and (A.25), inspired by the analysis of functionally graded materials (Aboudi et al., 1999), for the finite deformation of composites that consist of some rubber-like phases. In this case the repeating unit cell extends initially over $0 \leqslant Y_1 \leqslant D$, $0 \leqslant Y_2 \leqslant H$ and $0 \leqslant Y_3 \leqslant L$ in terms of the local material coordinates (Y_1, Y_2, Y_3) as stated above. The microstructure of the composite on the local level is modeled by discretizing the repeating unit cell into N_p, N_q and N_r generic cells in the intervals $0 \leqslant Y_1 \leqslant D$, $0 \leqslant Y_2 \leqslant H$ and $0 \leqslant Y_3 \leqslant L$, respectively, where a typical generic cell is shown see Fig. 1(c). As is illustrated in Fig. 1(c), a generic (p,q,r) cell consists of eight subcells designated by the triplet $(\alpha\beta\gamma)$ where each index takes the values 1 or 2, which indicate the relative position of the given subcell with respect to the local coordinates. The indices p, q and r, whose ranges are $p = 1, 2, \ldots, N_p$; $q = 1, 2, \ldots, N_q$ and $r = 1, 2, \ldots, N_r$, identify the generic cell in the Y_i space. The dimensions of the generic cell along the Y_1, Y_2 and Y_3 axes are $d_1^{(p)}$, $d_2^{(p)}$, $h_1^{(q)}$, $h_2^{(q)}$ and $l_1^{(r)}$, $l_2^{(r)}$, such that

$$D = \sum_{p=1}^{N_p}\left(d_1^{(p)} + d_2^{(p)}\right)$$

$$H = \sum_{q=1}^{N_q}\left(h_1^{(q)} + h_2^{(q)}\right)$$

$$L = \sum_{r=1}^{N_r}\left(l_1^{(r)} + l_2^{(r)}\right)$$

An approximate solution for the rates of displacement and temperature field is constructed based on volumetric averaging of the field equations together with the imposition of the periodic boundary conditions and continuity conditions in an average sense between the subcells used to characterize the materials' microstructure. This is accomplished by approximating the fluctuating displacement and the induced temperature rates in each subcell using a quadratic expansion in terms of local coordinates $\overline{\mathbf{Y}}^{(\alpha)}$, $\overline{\mathbf{Y}}^{(\beta)}$, $\overline{\mathbf{Y}}^{(\gamma)}$

centered at the subcell's midpoint. A higher order representation of the fluctuating displacement and the induced temperature rates is necessary in order to capture the local effects created by the field gradients and the microstructure of the composite. This is in sharp contrast with the so called generalized method of cells where the displacement increment expansion was linear (see Aboudi, 2001a).

With the above objective in mind, the fluctuating field in the subcell $(\alpha\beta\gamma)$ of the (p,q,r)th generic cell is approximated by a second-order expansion in the local coordinates system. Consequently, according to Eq. (10) the displacement rates in the subcell can be represented in the form (the generic cell label (p,q,r) has been omitted)

$$\dot{u}_i^{(\alpha\beta\gamma)} = \dot{\overline{F}}_{ij}X_j + \dot{W}_{i(000)}^{(\alpha\beta\gamma)} + \overline{Y}_1^{(\alpha)}\dot{W}_{i(100)}^{(\alpha\beta\gamma)} + \overline{Y}_2^{(\beta)}\dot{W}_{i(010)}^{(\alpha\beta\gamma)} + \overline{Y}_3^{(\gamma)}\dot{W}_{i(001)}^{(\alpha\beta\gamma)} + \frac{1}{2}\left(3\overline{Y}_1^{(\alpha)2} - \frac{d_\alpha^{(p)2}}{4}\right)\dot{W}_{i(200)}^{(\alpha\beta\gamma)} + \frac{1}{2}\left(3\overline{Y}_2^{(\beta)2} - \frac{h_\beta^{(q)2}}{4}\right)\dot{W}_{i(020)}^{(\alpha\beta\gamma)} + \frac{1}{2}\left(3\overline{Y}_3^{(\gamma)2} - \frac{l_\gamma^{(r)2}}{4}\right)\dot{W}_{i(002)}^{(\alpha\beta\gamma)} \tag{28}$$

where $\dot{W}_{i(000)}^{(\alpha\beta\gamma)}$, which are the rates of the fluctuating volume-averaged displacements, and the higher-order terms $\dot{W}_{i(lmn)}^{(\alpha\beta\gamma)}$ $(i = 1\text{–}3)$ must be determined, as shown below, from the coupled governing equation (17) as well as the periodic boundary conditions (18)–(20) that the fluctuating mechanical and induced thermal fields must fulfill, in conjunction with the interfacial continuity conditions between subcells.

Similarly, the following expansion for the rate of induced temperature is adopted:

$$\dot{\theta}^{(\alpha\beta\gamma)} = \dot{\theta}_{(000)}^{(\alpha\beta\gamma)} + \overline{Y}_1^{(\alpha)}\dot{\theta}_{(100)}^{(\alpha\beta\gamma)} + \overline{Y}_2^{(\beta)}\dot{\theta}_{(010)}^{(\alpha\beta\gamma)} + \overline{Y}_3^{(\gamma)}\dot{\theta}_{(001)}^{(\alpha\beta\gamma)} + \frac{1}{2}\left(3\overline{Y}_1^{(\alpha)2} - \frac{d_\alpha^{(p)2}}{4}\right)\dot{\theta}_{(200)}^{(\alpha\beta\gamma)} + \frac{1}{2}\left(3\overline{Y}_2^{(\beta)2} - \frac{h_\beta^{(q)2}}{4}\right)\dot{\theta}_{(020)}^{(\alpha\beta\gamma)} + \frac{1}{2}\left(3\overline{Y}_3^{(\gamma)2} - \frac{l_\gamma^{(r)2}}{4}\right)\dot{\theta}_{(002)}^{(\alpha\beta\gamma)} \tag{29}$$

It is readily seen that the total number of unknowns that describe the rates of the fluctuating displacements and induced temperature in the generic cell (p,q,r) is 224.

The rates of the deformation gradients are given by (7), in conjunction with (8) and (9), namely

$$\dot{F}_{ij}^{(\alpha\beta\gamma)} = \dot{\overline{F}}_{ij} + \partial_i \dot{u}_j^{(\alpha\beta\gamma)} \tag{30}$$

where $\partial_1 = \partial/\partial\overline{Y}_1^{(\alpha)}$, $\partial_2 = \partial/\partial\overline{Y}_2^{(\beta)}$ and $\partial_3 = \partial/\partial\overline{Y}_3^{(\gamma)}$.

In the course of satisfying the governing equations in a volumetric sense, it is convenient to define the following stress rate quantities in the subcell $(\alpha\beta\gamma)$ of generic cell (p,q,r):

$$\left[\dot{\mathbf{S}}_{(l,m,n)}^{(\alpha\beta\gamma)}\right]^{(p,q,r)} = \frac{1}{d_\alpha^{(p)}h_\beta^{(q)}l_\gamma^{(r)}}\int_{-d_\alpha^{(p)}/2}^{d_\alpha^{(p)}/2}\int_{-h_\beta^{(q)}/2}^{h_\beta^{(q)}/2}\int_{-l_\gamma^{(r)}/2}^{l_\gamma^{(r)}/2}\left(\overline{Y}_1^{(\alpha)}\right)^l\left(\overline{Y}_2^{(\beta)}\right)^m\left(\overline{Y}_3^{(\gamma)}\right)^n\dot{\mathbf{T}}^{(\alpha\beta\gamma)}\,\mathrm{d}\overline{Y}_1^{(\alpha)}\,\mathrm{d}\overline{Y}_2^{(\beta)}\,\mathrm{d}\overline{Y}_3^{(\gamma)} \tag{31}$$

For $l = m = n = 0$, Eq. (31) provides the average stress rates in the subcell, whereas for other values of (l,m,n) higher order values are obtained that are needed to describe the governing field equations of the continuum. These quantities can be evaluated explicitly in terms of the unknown coefficients $\dot{W}_{i(lmn)}^{(\alpha\beta\gamma)}$ and $\dot{\theta}_{(lmn)}^{(\alpha\beta\gamma)}$ by performing the required volume integration upon substituting Eqs. (12) and (30) and (28) and (29) in Eq. (31).

Similarly, we define in terms of the heat flux $\mathbf{q}^{(\alpha\beta\gamma)}$ in the subcell the following quantities:

$$\left[\mathbf{Q}_{(l,m,n)}^{(\alpha\beta\gamma)}\right]^{(p,q,r)} = \frac{1}{d_\alpha^{(p)}h_\beta^{(q)}l_\gamma^{(r)}}\int_{-d_\alpha^{(p)}/2}^{d_\alpha^{(p)}/2}\int_{-h_\beta^{(q)}/2}^{h_\beta^{(q)}/2}\int_{-l_\gamma^{(r)}/2}^{l_\gamma^{(r)}/2}\left(\overline{Y}_1^{(\alpha)}\right)^l\left(\overline{Y}_2^{(\beta)}\right)^m\left(\overline{Y}_3^{(\gamma)}\right)^n\mathbf{q}^{(\alpha\beta\gamma)}\,\mathrm{d}\overline{Y}_1^{(\alpha)}\,\mathrm{d}\overline{Y}_2^{(\beta)}\,\mathrm{d}\overline{Y}_3^{(\gamma)} \tag{32}$$

These quantities can be evaluated explicitly by substituting the integrated coefficients $\theta_{(lmn)}^{(\alpha\beta\gamma)}$ in Eq. (A.27) and performing the required volume integration of Eq. (32).

Subsequently, satisfaction of the zeroth, first, and second moments of the equilibrium, Eq. (17) results in the following 24 relations among the the volume-averaged first-order field values $\dot{\mathbf{S}}^{(\alpha\beta\gamma)}_{(l,m,n)}$ in the different subcells $(\alpha\beta\gamma)$ of the (p,q,r) generic cell, after lengthy algebraic manipulations

$$\left[\dot{S}^{(\alpha\beta\gamma)}_{1j(1,0,0)}/d_\alpha^2+\dot{S}^{(\alpha\beta\gamma)}_{2j(0,1,0)}/h_\beta^2+\dot{S}^{(\alpha\beta\gamma)}_{3j(0,0,1)}/l_\gamma^2\right]^{(p,q,r)}=0\quad j=1\text{–}3 \tag{33}$$

Similarly, the satisfaction of the zeroth, first, and second moments of the energy equation (A.25) results, after lengthy algebraic manipulations, in the following eight relations

$$\left[(\rho c_v)^{(\alpha\beta\gamma)}\left\{\dot{\theta}^{(\alpha\beta\gamma)}_{(000)}-\frac{d_\alpha^2}{20}\dot{\theta}^{(\alpha\beta\gamma)}_{(200)}-\frac{h_\beta^2}{20}\dot{\theta}^{(\alpha\beta\gamma)}_{(020)}-\frac{l_\gamma^2}{20}\dot{\theta}^{(\alpha\beta\gamma)}_{(002)}\right\}+B^{(\alpha\beta\gamma)}_{ik}\left(\dot{\bar{F}}_{ki}+\dot{\tilde{F}}^{(\alpha\beta\gamma)}_{ki(000)}\right)\right.$$
$$\left.-\frac{1}{d_\alpha^2}Q^{(\alpha\beta\gamma)}_{1(1,0,0)}-\frac{1}{h_\beta^2}Q^{(\alpha\beta\gamma)}_{2(0,1,0)}-\frac{1}{l_\gamma^2}Q^{(\alpha\beta\gamma)}_{3(0,0,1)}\right]^{(p,q,r)}=0 \tag{34}$$

where $\dot{\tilde{F}}^{(\alpha\beta\gamma)}_{ki(000)}$ is obtained from the material derivatives of $\dot{u}_i^{(\alpha\beta\gamma)}$ given by (28).

The continuity of traction at the subcell interfaces and between adjacent generic cells, imposed in an average sense, in the 1-direction can be shown to be ensured by the following relations:

$$\left[-12\dot{S}^{(1\beta\gamma)}_{1j(1,0,0)}/d_1+\dot{S}^{(2\beta\gamma)}_{1j(0,0,0)}-6\dot{S}^{(2\beta\gamma)}_{1j(1,0,0)}/d_2\right]^{(p,q,r)}-\left[\dot{S}^{(2\beta\gamma)}_{1j(0,0,0)}+6\dot{S}^{(2\beta\gamma)}_{1j(1,0,0)}/d_2\right]^{(p-1,q,r)}=0 \tag{35}$$

and

$$\left[-\dot{S}^{(1\beta\gamma)}_{1j(0,0,0)}+\frac{1}{2}\dot{S}^{(2\beta\gamma)}_{1j(0,0,0)}-3\dot{S}^{(2\beta\gamma)}_{1j(1,0,0)}/d_2\right]^{(p,q,r)}+\frac{1}{2}\left[\dot{S}^{(2\beta\gamma)}_{1j(0,0,0)}+6\dot{S}^{(2\beta\gamma)}_{1j(1,0,0)}/d_2\right]^{(p-1,q,r)}=0 \tag{36}$$

Similarly, the continuity of heat flux at the subcell interfaces and between adjacent generic cells, imposed in an average sense, in the 1-direction can be shown to be ensured by

$$\left[(\rho c_v)^{(1\beta\gamma)}\frac{d_1^3}{20}\dot{\theta}^{(1\beta\gamma)}_{(200)}-\frac{12}{d_1}Q^{(1\beta\gamma)}_{1(1,0,0)}\right]^{(p,q,r)}+\left[(\rho c_v)^{(2\beta\gamma)}\frac{d_2^3}{40}\dot{\theta}^{(2\beta\gamma)}_{(200)}-\frac{6}{d_2}Q^{(2\beta\gamma)}_{1(1,0,0)}\right]^{(p,q,r)}$$
$$+\left[(\rho c_v)^{(2\beta\gamma)}\frac{d_2^3}{40}\dot{\theta}^{(2\beta\gamma)}_{(200)}-\frac{6}{d_2}Q^{(2\beta\gamma)}_{1(1,0,0)}\right]^{(p-1,q,r)}-\left[(\rho c_v)^{(2\beta\gamma)}\frac{d_2^2}{12}\dot{\theta}^{(2\beta\gamma)}_{(100)}+\frac{d_2^2}{12}B^{(2\beta\gamma)}_{ik}\left(\dot{\bar{F}}_{ki}+\dot{\tilde{F}}^{(2\beta\gamma)}_{ki(100)}\right)-Q^{(2\beta\gamma)}_{1(0,0,0)}\right]^{(p,q,r)}$$
$$+\left[(\rho c_v)^{(2\beta\gamma)}\frac{d_2^2}{12}\dot{\theta}^{(2\beta\gamma)}_{(100)}+\frac{d_2^2}{12}B^{(2\beta\gamma)}_{ik}\left(\dot{\bar{F}}_{ki}+\dot{\tilde{F}}^{(2\beta\gamma)}_{ki(100)}\right)-Q^{(2\beta\gamma)}_{1(0,0,0)}\right]^{(p-1,q,r)}=0 \tag{37}$$

and

$$\left[(\rho c_v)^{(1\beta\gamma)}\frac{d_1^2}{12}\dot{\theta}^{(1\beta\gamma)}_{(100)}+\frac{d_1^2}{4}B^{(1\beta\gamma)}_{ik}\left(\dot{\bar{F}}_{ki}+\dot{\tilde{F}}^{(1\beta\gamma)}_{ki(100)}\right)-Q^{(1\beta\gamma)}_{1(0,0,0)}\right]^{(p,q,r)}-\left[(\rho c_v)^{(2\beta\gamma)}\frac{d_1^2}{24}\dot{\theta}^{(2\beta\gamma)}_{(100)}+\frac{d_2^2}{8}B^{(2\beta\gamma)}_{ik}\left(\dot{\bar{F}}_{ki}+\dot{\tilde{F}}^{(2\beta\gamma)}_{ki(100)}\right)\right.$$
$$\left.-\frac{1}{2}Q^{(2\beta\gamma)}_{1(0,0,0)}\right]^{(p,q,r)}-\left[(\rho c_v)^{(2\beta\gamma)}\frac{d_1^2}{24}\dot{\theta}^{(2\beta\gamma)}_{(100)}+\frac{d_2^2}{8}B^{(2\beta\gamma)}_{ik}\left(\dot{\bar{F}}_{ki}+\dot{\tilde{F}}^{(2\beta\gamma)}_{ki(100)}\right)-\frac{1}{2}Q^{(2\beta\gamma)}_{1(0,0,0)}\right]^{(p-1,q,r)}$$
$$+\left[(\rho c_v)^{(2\beta\gamma)}\frac{d_2^3}{80}\dot{\theta}^{(2\beta\gamma)}_{(200)}-\frac{3}{d_2}Q^{(2\beta\gamma)}_{1(1,0,0)}\right]^{(p,q,r)}-\left[(\rho c_v)^{(2\beta\gamma)}\frac{d_2^3}{80}\dot{\theta}^{(2\beta\gamma)}_{(200)}-\frac{3}{d_2}Q^{(2\beta\gamma)}_{1(1,0,0)}\right]^{(p-1,q,r)}=0 \tag{38}$$

The continuity of traction and heat flux in the 2- and 3-directions generate similar conditions which need not be given here. Eqs. (35)–(38) and the corresponding ones in the 2-and 3-direction provide altogether 144 additional relations among the zeroth-order, first-order and second-order field quantities in the generic cell (p,q,r).

The additional 48 relations necessary to determine the unknown coefficients in the field expansion are obtained by imposing displacement and temperature continuity conditions on an average basis at each subcell and cell interface. In the 1-direction this produces,

$$\left[\dot{W}_{i(000)}^{(1\beta\gamma)}+\frac{1}{2}d_1\dot{W}_{i(100)}^{(1\beta\gamma)}+\frac{1}{4}d_1^2\dot{W}_{i(200)}^{(1\beta\gamma)}\right]^{(p,q,r)}=\left[\dot{W}_{i(000)}^{(2\beta\gamma)}-\frac{1}{2}d_2\dot{W}_{i(100)}^{(2\beta\gamma)}+\frac{1}{4}d_2^2\dot{W}_{i(200)}^{(2\beta\gamma)}\right]^{(p,q,r)} \tag{39}$$

$$\left[\dot{W}_{i(000)}^{(2\beta\gamma)}+\frac{1}{2}d_2\dot{W}_{i(100)}^{(2\beta\gamma)}+\frac{1}{4}d_2^2\dot{W}_{i(200)}^{(2\beta\gamma)}\right]^{(p,q,r)}=\left[\dot{W}_{i(000)}^{(1\beta\gamma)}-\frac{1}{2}d_1\dot{W}_{i(100)}^{(1\beta\gamma)}+\frac{1}{4}d_1^2\dot{W}_{i(200)}^{(1\beta\gamma)}\right]^{(p+1,q,r)} \tag{40}$$

with $i = 1$–3, and

$$\left[\dot{\theta}_{(000)}^{(1\beta\gamma)}+\frac{1}{2}d_1\dot{\theta}_{(100)}^{(1\beta\gamma)}+\frac{1}{4}d_1^2\dot{\theta}_{(200)}^{(1\beta\gamma)}\right]^{(p,q,r)}=\left[\dot{\theta}_{(000)}^{(2\beta\gamma)}-\frac{1}{2}d_2\dot{\theta}_{(100)}^{(2\beta\gamma)}+\frac{1}{4}d_2^2\dot{\theta}_{(200)}^{(2\beta\gamma)}\right]^{(p,q,r)} \tag{41}$$

$$\left[\dot{\theta}_{(000)}^{(2\beta\gamma)}+\frac{1}{2}d_2\dot{\theta}_{(100)}^{(2\beta\gamma)}+\frac{1}{4}d_2^2\dot{\theta}_{(200)}^{(2\beta\gamma)}\right]^{(p,q,r)}=\left[\dot{\theta}_{(000)}^{(1\beta\gamma)}-\frac{1}{2}d_1\dot{\theta}_{(100)}^{(1\beta\gamma)}+\frac{1}{4}d_1^2\dot{\theta}_{(200)}^{(1\beta\gamma)}\right]^{(p+1,q,r)} \tag{42}$$

Similar relations hold in the 2- and 3-directions which are not given here. All these relations provide the required 48 additional equations.

Thus, the equilibrium and energy equations together with the continuity of traction, heat flux, displacement, and temperature form 224 equations in the 224 unknowns rate of field variables in any interior generic cell (p,q,r), $p = 2,\ldots,N_p-1$, $q = 2,\ldots,N_q-1$ and $r = 2,\ldots,N_r-1$. For the boundary cells $p = 1$, N_p, $q = 1$, N_q and $r = 1$, N_r a different treatment must be applied.

For generic cell $(1,q,r)$, for example, the above relations are operative, except Eqs. (35)–(38), which follow from the continuity of traction and heat flux between a given cell and the preceding one. These equations must be replaced by the conditions of continuity of traction and heat flux at the interior interfaces of cell $(1,q,r)$ (imposed on the average sense), and by the conditions that the fluctuating displacements, and the induced temperature are periodic. For example the periodicity of the displacement in the 1-direction provides (see the first relation in Eq. (18))

$$\left[\dot{W}_{i(000)}^{(1\beta\gamma)}-\frac{1}{2}d_1\dot{W}_{i(100)}^{(1\beta\gamma)}+\frac{1}{4}d_1^2\dot{W}_{i(200)}^{(1\beta\gamma)}\right]^{(1,q,r)}=\left[\dot{W}_{i(000)}^{(2\beta\gamma)}+\frac{1}{2}d_2\dot{W}_{i(100)}^{(2\beta\gamma)}+\frac{1}{4}d_2^2\dot{W}_{i(200)}^{(2\beta\gamma)}\right]^{(N_p,q,r)} \tag{43}$$

where $i = 1$–3. Similar treatments apply for cell $(p,1,r)$ and $(p,q,1)$.

For the boundary generic cell (N_p,q,r), for example, the previously derived governing equations are operative except for the relations given by Eqs. (40) and (42), which are obviously not applicable. These are replaced by the conditions that the tractions and heat fluxes are periodic. For example the periodicity of tractions provide the following equations to be used in cell (N_p,q,r) (see the second relation in Eq. (18))

$$\left[\frac{6}{d_1}\dot{S}_{1j(1,0,0)}^{(1\beta\gamma)}-\dot{S}_{1j(0,0,0)}^{(1\beta\gamma)}\right]^{(1,q,r)}+\left[\frac{6}{d_2}\dot{S}_{1j(1,0,0)}^{(2\beta\gamma)}+\dot{S}_{1j(0,0,0)}^{(2\beta\gamma)}\right]^{(N_p,q,r)}=0 \tag{44}$$

Similar treatments hold for boundary cells (p,N_q,r) and (p,q,N_r).

Consequently, the governing equations for the interior and boundary cells form a linear system of 224 $N_pN_qN_r$ algebraic equations in the unknown field coefficient rates that appear in the quadratic expansions (28) and (29). The final form of this system of equations can be symbolically represented by

$$\mathbf{K}\dot{\mathbf{U}}=\mathbf{f} \tag{45}$$

where the structural stiffness matrix $\mathbf{K}$ contains information on the geometry and the properties of the materials within the individual subcells $(\alpha\beta\gamma)$ within the generic cells comprising the repeating unit cell of

multiphase periodic composite. The field vector $\dot{\mathbf{U}}$ contains the unknown expansion coefficients in each subcell, i.e.,

$$\dot{\mathbf{U}} = \frac{\partial}{\partial t}\left[\mathbf{U}_{111}^{(111)}, \ldots, \mathbf{U}_{N_pN_qN_r}^{(222)}\right] \tag{46}$$

where in subcell $(\alpha\beta\gamma)$ of generic cell (p,q,r) these coefficients are

$$\mathbf{U}_{pqr}^{(\alpha\beta\gamma)} = \left[W_{i(000)}, W_{i(100)}, W_{i(010)}, W_{i(001)}, W_{i(200)}, W_{i(020)}, W_{i(002)}, \theta_{(000)}, \theta_{(100)}, \theta_{(010)}, \theta_{(001)}, \theta_{(200)}, \theta_{(020)}, \theta_{(002)}\right]_{pqr}^{(\alpha\beta\gamma)}$$
$$i = 1\text{–}3$$

The force vector $\mathbf{f}$ contains information on the rate of applied average displacement gradient $\dot{\overline{\mathbf{F}}}$ and the current displacement and temperature microvariables. The solution that establishes the response of the composite is obtained incrementally in time by solving Eq. (45) for the rates of microvariables at a given time t, from which the microvariables are determined by a simple Eulerian integration.

6. Global constitutive relations

Once the solution $\dot{\mathbf{U}}$ for a given set of average deformation gradient rates has been established at a given load increment, we can determine, in particular, the average displacement gradient and temperature rates in all subcells via the corresponding concentration tensors, see Eqs. (23) and (24). Thus, the rate of average stress $[\dot{\mathbf{S}}_{(0,0,0)}^{(\alpha\beta\gamma)}]^{(p,q,r)}$ in subcell $(\alpha\beta\gamma)$ of the generic cell (p,q,r) are given by

$$\left[\dot{\mathbf{S}}_{(0,0,0)}^{(\alpha\beta\gamma)}\right]^{(p,q,r)} = \left[\left(\mathbf{R}^{(\alpha\beta\gamma)}\mathbf{A}^{(\alpha\beta\gamma)} - \mathbf{H}^{(\alpha\beta\gamma)}\mathbf{a}^{(\alpha\beta\gamma)}\right)\right]^{(p,q,r)}\dot{\overline{\mathbf{F}}} \tag{47}$$

The average stress rate in the multiphase periodic composite is determined from

$$\dot{\overline{\mathbf{T}}} = \frac{1}{DHL}\sum_{p=1}^{N_p}\sum_{q=1}^{N_q}\sum_{r=1}^{N_r}\sum_{\alpha,\beta,\gamma=1}^{2} d_\alpha^{(p)} h_\beta^{(q)} l_\gamma^{(r)}\left[\dot{\mathbf{S}}_{(0,0,0)}^{(\alpha\beta\gamma)}\right]^{(p,q,r)} \tag{48}$$

Consequently, Eqs. (47) and (48) establish the effective constitutive law of the multiphase composite in the form

$$\dot{\overline{\mathbf{T}}} = \mathbf{R}^*\dot{\overline{\mathbf{F}}} \tag{49}$$

where $\mathbf{R}^*$ is the instantaneous effective stiffness tensor of the composite which is given by

$$\mathbf{R}^* = \frac{1}{DHL}\sum_{p=1}^{N_p}\sum_{q=1}^{N_q}\sum_{r=1}^{N_r}\sum_{\alpha,\beta,\gamma=1}^{2} d_\alpha^{(p)} h_\beta^{(q)} l_\gamma^{(r)}\left[\mathbf{R}^{(\alpha\beta\gamma)}\mathbf{A}^{(\alpha\beta\gamma)} - \mathbf{H}^{(\alpha\beta\gamma)}\mathbf{a}^{(\alpha\beta\gamma)}\right]^{(p,q,r)} \tag{50}$$

7. Applications

The predictive capability of the derived micromechanical analysis is demonstrated by its application to composite materials with rubber-like matrix reinforced by nylon fibers. The material properties of a thermoelastic vulcanized rubber at a reference temperature $\theta_0 = 293$ K are given in Table 1. The nylon constituent is assumed to be linearly elastic with Young's modulus, Poisson's ratio, coefficient of thermal expansion, mass density, specific heat at constant deformation and thermal conductivity given, respectively, by (Perry, 1963): 2 GPa, 0.4, 90×10^{-6}/K, 1140 kg/m^3, 1675 J/(kg K), 0.24 W/(mK). It should be empha-

Table 1
Material properties of vulcanized rubber at $\theta_0 = 293$ K (Chadwick, 1974; Morman, 1995)

Property	Value
ρ_0	906.5 kg/m^3
c_v	1662 J/(kg K)
κ_0	0.2 W/(mK)
κ	1950 MPa
μ	0.98 MPa
m	9
n	2.5
γ	1/6
α_0	657×10^{-6}/K
c_{10}	0.2357 MPa
c_{01}	0.2426 MPa
c_{11}	−0.567 kPa
c_{20}	7.41 kPa
c_{30}	0.0464 kPa

sized that the present micromechanical theory is capable of handling the nonlinear thermoelastic behavior of the nylon cords. In the absence of a reliable nonlinear constitutive law for nylon, however, a linear behavior has been assumed. Results are given for nylon/rubber-like matrix composites that are subjected to (1) thermal loading with prescribed extension and (2) thermal loading with prescribed stress, in both of which there is no thermomechanical coupling. Results are also given for applied hydrostatic, axial, transverse and biaxial transverse mechanical loadings in which full coupling exists. The results provided by the present theory, with full thermomechanical coupling, were compared in the special case of linearly elastic phases with those previously obtained by Williams and Aboudi (1999) and excellent agreements exist.

7.1. Isometric behavior: thermal loading with prescribed extensions

We start with the one-way coupling situation in which the temperature is prescribed in advance and the resulting mechanical response is sought. Consider a unidirectional nylon/rubber-like matrix composite in which the nylon cords are oriented in the 1-direction. The composite is subjected to a thermal loading according to which the temperature is incrementally increased from θ_0 by 100 K. In addition, the composite is subjected to prescribed transverse stretches in the 2-direction whose values are $\lambda_2 = 1.01$, 1.1 and 1.2. The resulting stress-temperature response is shown in Fig. 2 for a homogeneous (unreinforced) rubber-like matrix ($v_f = 0$) and unidirectional composites with fiber volume fractions $v_f = 0.25$ and 0.5. At the lower and intermediate value of $\bar{\lambda}_2$ the matrix exhibits the ordinary behavior in which the stress gradient is negative. At the highest value of the applied stretch this gradient is positive, clearly exhibiting the thermoelastic inversion effect. This behavior is seen to take place in the composite with the lower volume fraction. For the unidirectional composite with $v_f = 0.5$, on the other hand, this effect is seen to occur at stretch values $\bar{\lambda}_2 = 1.1$ and 1.2. Thus the amount of fiber reinforcement has a significant influence on the thermoelastic inversion effect that is exhibited by rubber-like matrix composites.

7.2. Isotonic behavior: thermal loading with prescribed stresses

Here too the one-way coupling case is considered in which the same unidirectional nylon/rubber-like matrix composite with nylon fibers oriented in the 1-direction, is subjected to thermal loading according to which the temperature is incrementally increased from θ_0 by 100 K. Presently, the composite is also

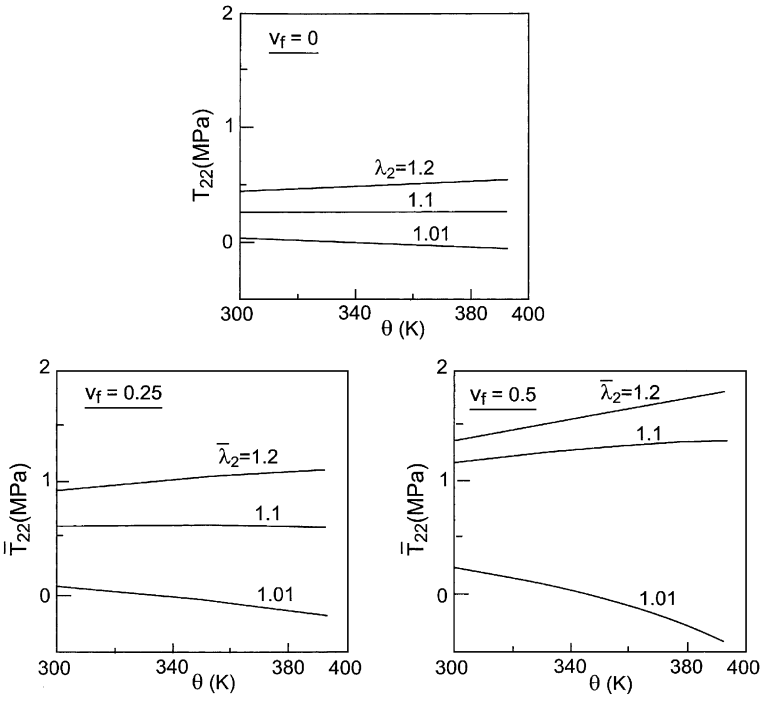

Fig. 2. Stress–temperature response of homogeneous matrix ($v_f = 0$) and unidirectional nylon/rubber composite with fiber volume fractions $v_f = 0.25$ and 0.5, that are subjected to three values of prescribed stretches in the transverse 2-direction.

subjected to a prescribed transverse stress $\overline{T}_{22}$ in the 2-direction of 0.1, 0.5 and 0.75 MPa. The resulting stretch-temperature responses are shown in Fig. 3 for a homogeneous rubber-like matrix ($v_f = 0$) and unidirectional composites with fiber volume fractions $v_f = 0.25$ and 0.5. The case with applied stress of 0.1 MPa exhibits the ordinary response where the stretch gradient with respect to the temperature is positive. Negative gradients are exhibited by the matrix for $T_{22} = 0.5$ and 0.75 MPa. But for the unidirectional composite this negative gradient is exhibited only in the case with a fiber volume fraction of $v_f = 0.25$. All other situations considered show positive gradients. The decreasing magnitudes of the stretches with increasing volume fraction should be noted. This behavior is contrary to the case of thermal loading with prescribed stretches that was shown in Fig. 2, where the induced stresses increased with increase of fiber volume fraction.

7.3. Hydrostatic loading

In order to exhibit the effect of full thermomechanical coupling, we consider the rubber-like (unreinforced) matrix material that is subjected to a hydrostatic loading $\lambda_1 = \lambda_2 = \lambda_3$. The resulting stress $T_{11} = T_{22} = T_{33}$ and the induced temperature deviation $\Delta\theta = \theta - \theta_0$ are shown in Fig. 4. Also shown in the figure is the uncoupled case in which the induced temperature due to the applied mechanical loading obviously vanishes. It is clearly observed that the effect of coupling is appreciable and cannot be ignored in the present case. It should be mentioned that in the hypothetical case in which the rubber is assumed to behave as a linearly elastic material, the induced temperature deviation due to a hydrostatic loading is $\Delta\theta = -250\epsilon_{kk}$ (ϵ_{kk} denotes the small strain component). Thus the effect of nonlinearity is significant as can

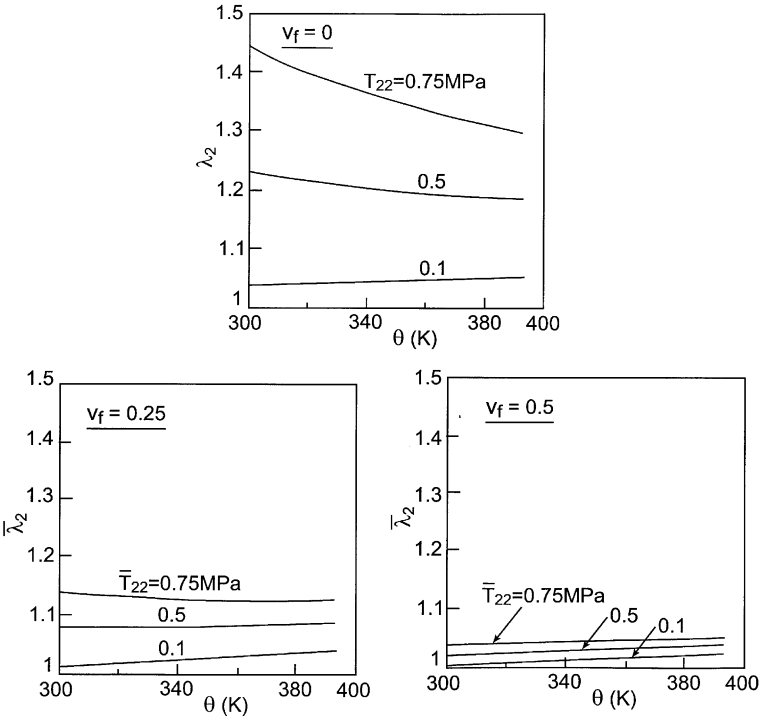

Fig. 3. Stretch–temperature response of homogeneous matrix ($v_f = 0$) and unidirectional nylon/rubber composite with fiber volume fractions $v_f = 0.25$ and 0.5, that are subjected to three values of prescribed normal stresses in the transverse 2-direction.

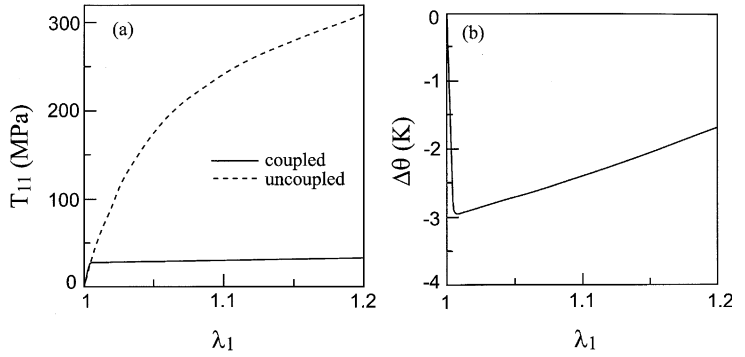

Fig. 4. (a) Stress–stretch response of homogeneous (unreinforced) matrix, and (b) the induced temperature deviation, due to an applied hydrostatic loading.

be observed from Fig. 4(a) where the stress response exhibits a strongly nonlinear curve and from Fig. 4(b) that shows a very small temperature deviation (as compared to the linear case).

Consider next a particulate nylon/rubber-like matrix composite that is subjected to a hydrostatic loading such that the applied principal stretches are $\bar{\lambda}_1 = \bar{\lambda}_2 = \bar{\lambda}_3$. The resulting response is depicted in Fig. 5 as the stress $\overline{T}_{11} = \overline{T}_{22} = \overline{T}_{33}$ against the applied stretches. Also shown is the average of the induced temperature $\Delta\bar{\theta} = \bar{\theta} - \theta_0$ ($\bar{\theta}$ is the average of the temperatures induced in the fiber and matrix phases of the composite).

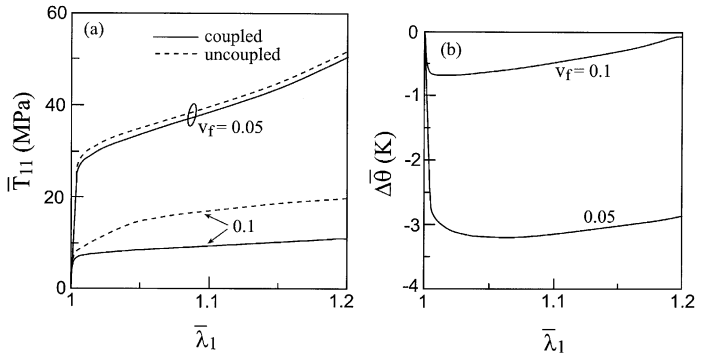

Fig. 5. (a) Stress–stretch response of a particulate nylon/rubber composite, and (b) the induced average temperature deviation, due to an applied hydrostatic loading for reinforcement volume fractions $v_f = 0.05$ and 0.1.

The figure shows this response for a composite with particle volume fraction $v_f = 0.05$ and 0.1 and also exhibits the effect of existing thermoelastic coupling. Since the considered rubber-like material is almost incompressible (see Table 1 according to which the bulk modulus is about 2000 times the shear modulus), the homogeneous matrix exhibits high stress values as it has been shown in Fig. 4. By introducing the nylon particles, the composite becomes compressible, and the values of the stresses decrease significantly as shown in Fig. 5. The amount of compressibility increases as the volume fraction increases. Furthermore, the introduction of the nylon phase results in a decrease of the induced temperature deviation. This can be anticipated from the fact that for monolithic linearly elastic nylon that is subjected to a hydrostatic loading, $\Delta\theta = -138\epsilon_{kk}$, which is lower than that induced in a linearly elastic rubber.

7.4. Axial loading

Let us consider the monolithic rubber-like material that is subjected to uniaxial stress loading. The coupling term in the linear energy equation is proportional to $\dot{\epsilon}_{kk}$. This implies that for a nearly incompressible material subjected to this type of loading, the induced temperature is very small, which is indeed the case. By introducing nylon fibers (in the 1-direction) the composite becomes compressible, with the amount of compressibility increasing with the fiber volume ratio v_f. In Fig. 6 the axial stress and the induced temperature deviation are shown for $v_f = 0.25$ and 0.5 for a nylon/rubber-like composite that is

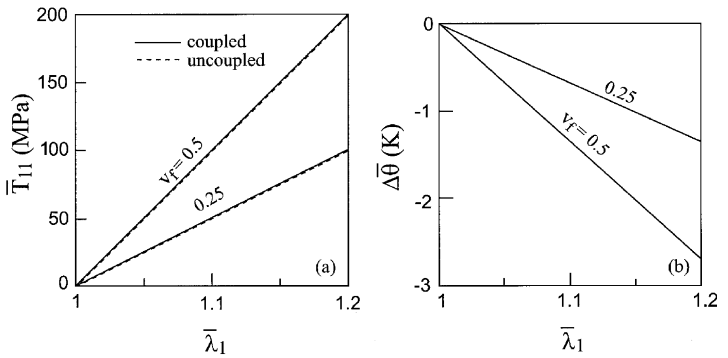

Fig. 6. (a) Axial stress–stretch response of a unidirectional nylon/rubber composite, and (b) the induced average temperature deviation, due to an applied uniaxial stress loading in the fiber direction for reinforcement volume fractions $v_f = 0.25$ and 0.5.

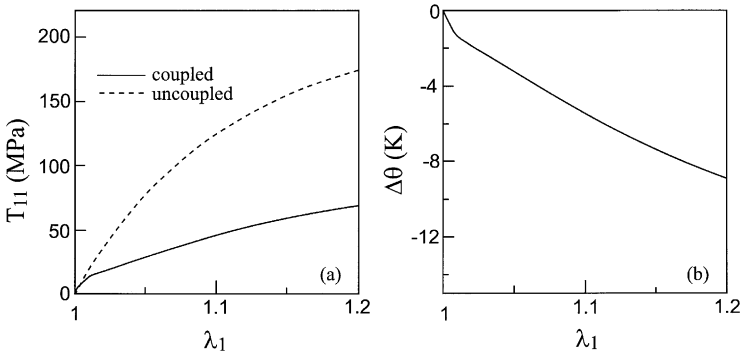

Fig. 7. (a) Stress–stretch response of homogeneous (unreinforced) matrix, and (b) the induced temperature deviation, due to an applied stretch loading in the 1-direction.

subjected to a uniaxial stress loading in the fiber direction. It is readily seen that the behavior of the composite is dominated by the much stiffer fibers, resembling a composite with linearly elastic phases (Williams and Aboudi, 1999). The mechanical response in the presence of the full thermomechanical coupling coincides with the response in the absence of such coupling. In both cases the response is dominated by the effective axial Young's modulus of the composite in the linear region, which is approximately given by $2v_f$ GPa (the Young's moduli of the nylon fiber and of the rubber-like matrix in the linear region are 2 GPa and 3 MPa, respectively).

In order to further study the effect of thermomechanical coupling, let us subject the monolithic rubber-like material to a uniaxial stretch in the 1-direction while keeping all other directions rigidly fixed. The resulting response and induced temperature are shown in Fig. 7. The resulting stresses are relatively high due to the highly incompressible material, and the effect of coupling is seen to be significant. Furthermore, taking into account that, in the hypothetical case of a linearly elastic material under this type of loading, the generated temperature deviation due to coupling would be $\Delta\theta = -250\epsilon_{11}$, it appears from Fig. 7 that effect of nonlinearity is pronounced.

Similarly, let us subject the unidirectional composite to a uniaxial stretch in the fiber direction (with all other directions kept rigidly fixed). The resulting response and induced temperature are shown in Fig. 8 for two values of fiber volume ratio. This figure shows that the effect of thermomechanical coupling decreases with increasing volume fraction, namely as the nylon phase becomes more dominant.

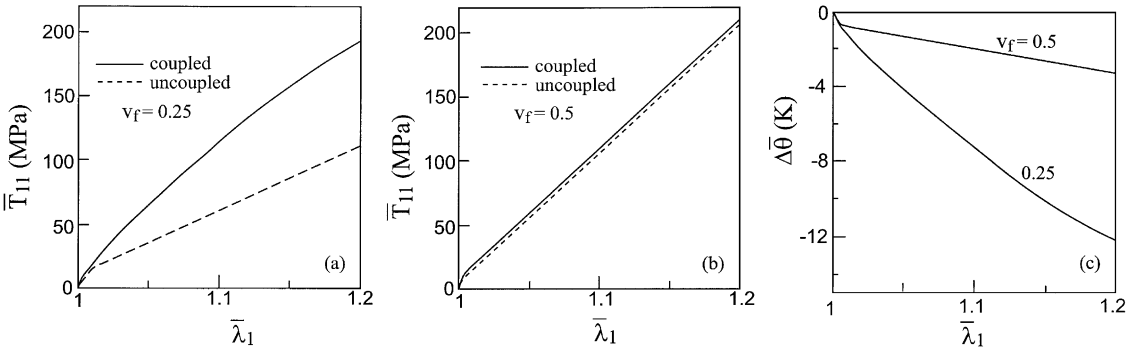

Fig. 8. (a) Axial stress–stretch response of a unidirectional nylon/rubber composite with fiber volume fraction $v_f = 0.25$, (b) $v_f = 0.5$, and (c) the induced average temperature deviation, due to an applied uniaxial stretch loading in the fiber direction.

7.5. Transverse loading

Since in the case of a transverse stress loading perpendicular to the fiber direction the behavior of the composite is essentially controlled by the matrix, the effect of thermoelastic coupling is very small due to the nearly incompressible matrix. Let us consider, therefore, a uniaxial stretch loading perpendicular to the fiber direction (i.e. loading in the transverse 2-direction) so that the effect of the incompressibility of the matrix is circumvented. The response to this type of loading is exhibited in Fig. 9. Here too the effect of thermomechanical coupling is more appreciable for the lower fiber volume fractions. The presently smaller values of the stresses and induced temperatures as compared with those previously obtained in Fig. 8 should be noted.

7.6. Biaxial transverse loading

Consider a homogeneous rubber-like material that is subjected to a biaxial stretch loading in the 2- and 3-directions. In the 1-direction the material is kept rigidly clamped. The response to the present type of loading is shown in Fig. 10. A comparison with Fig. 7 for a uniaxial stretch loading shows that the effect of thermomechanical coupling in the present case is more severe. This is manifested as a significant difference

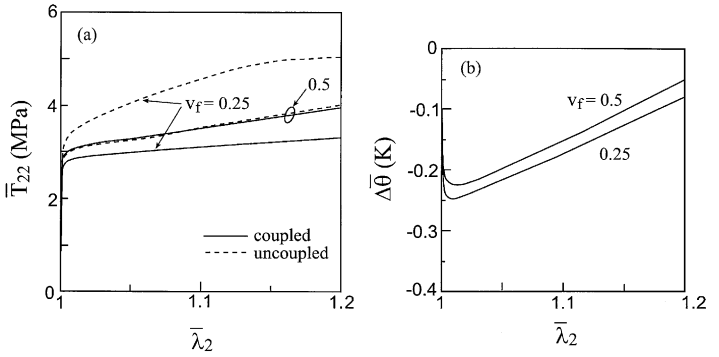

Fig. 9. (a) Transverse stress–stretch response of a unidirectional nylon/rubber composite with fiber volume fraction $v_f = 0.25$ and 0.5, and (b) the induced average temperature deviation, due to an applied uniaxial stretch loading perpendicular to the fiber direction.

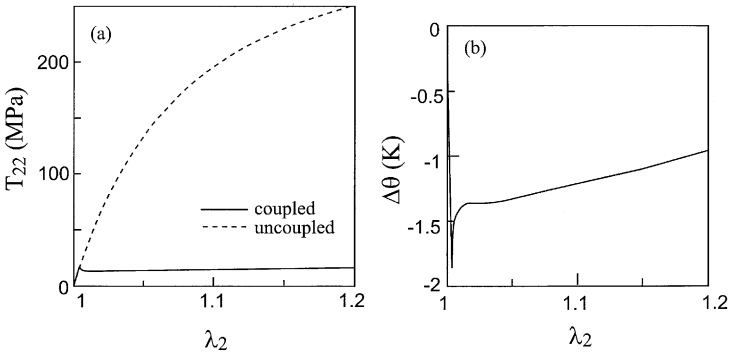

Fig. 10. (a) Stress–stretch response of homogeneous (unreinforced) matrix, and (b) the induced temperature deviation, due to an applied biaxial stretch loading in the 2- and 3-directions.

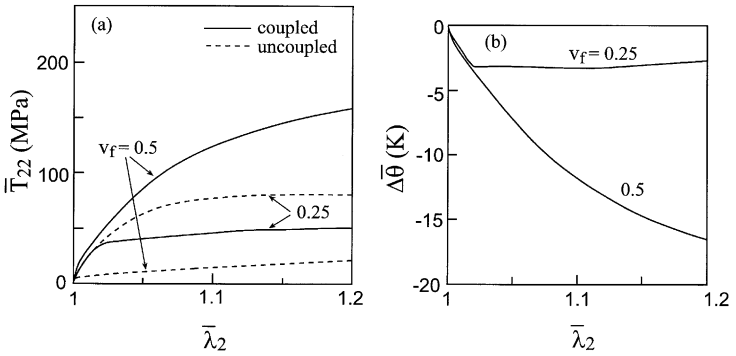

Fig. 11. (a) Transverse stress–stretch response of a unidirectional nylon/rubber composite with fiber volume fraction $v_f = 0.25$ and 0.5, and (b) the induced average temperature deviation, due to an applied biaxial stretch loading perpendicular to the fiber direction.

between the stresses generated in the coupled and uncoupled cases, as well as an induced temperature that is much smaller due to the strong coupling effects. Here too the effect of the nonlinear behavior of the matrix is seen to be significant in both the stress–stretch response and the induced temperature deviation.

Finally, the effect of biaxial stretching perpendicular to the fiber direction of the nylon/rubber-like composite is shown in Fig. 11. As in previous cases, the coupling effect appears to decrease with increasing fiber volume fraction. A comparison of this figure with Fig. 9 shows that the stress–stretch response and induced temperature due to the transverse combined loading appear to be far more complex than that caused by a simple transverse loading.

8. Conclusions

A micromechanical model based on the homogenization procedure has been derived and applied to investigate the effect of thermomechanical coupling that exists during the finite deformation of rubber-like matrix composites. This new micromechanical theory, which is based on a second-order expansion of the local displacements, has been previously implemented for the prediction of the effective thermoelastic moduli of unidirectional composites (assuming small strains) (Aboudi et al., 2001), and excellent agreement with several finite element solutions was demonstrated. In addition, the prediction of these moduli by the generalized method of cells (GMC) model (Aboudi, 1996), which is based on a linear expansion of local displacements, has been shown to agree well with finite element results. The accuracy of the local field which is predicted by the new micromechanical theory, was demonstrated in Aboudi et al. (2001) by comparisons with elasticity solution for an inclusion in an infinite matrix.

The new micromechanical theory presented herein has also been employed to predict the effective moduli of electro-magneto-thermo-elastic composites (Aboudi, 2001b). Extensive comparisons with the predictions provided by GMC and the results of Li and Dunn (1998) (that are based on the Mori and Tanaka (1973) model) exhibit excellent agreement.

In contrast with the present new micromechanical model however, GMC suffers from a lack of coupling between normal and shear effects. This absence of shear coupling in GMC (that results from the linear expansion assumption) has only a slight effect on the accuracy of the predicted effective moduli and the overall composite inelastic response, but GMC's estimate of the local field is less accurate. On the other hand, the excellent accuracy of the local field (in addition to the effective moduli) predicted by the new micromechanical theory, has been demonstrated in Aboudi et al. (2001, 2002) by performing extensive comparisons with analytical and finite element solutions under various circumstances (e.g., composites

under normal, axial shear and thermal loadings) in the presence and absence of inelastic effects. It can be concluded that whenever the effective moduli or the global constitutive law of inelastic composites are sought, the use of GMC model provides quite accurate results. When the accurate local field is needed, on the other hand (as, for example, in the case of a damage analysis of composites), the new micromechanical theory should be employed.

It should be mentioned that both the new approach and GMC have common features. Both models are suitable for the analysis of periodic multiphase composites and rely on the analysis of a repeating unit cell. Both these models are analytical and provide closed-form expressions for the effective stiffness tensor and for the overall eigenstrains (e.g. inelastic strains) of the composite. In both models, any type of simple or combined loading can be applied irrespective of whether symmetry exists or not, and without restoring to different boundary condition application strategies as required in the case of a finite element analysis of a repeating unit cell (which does not employ periodic boundary conditions). Due to the availability of analytical expressions representing the macroresponse of the composite, both models can be incorporated into a composite structural analysis computer code.

Finally, due to the absence of shear coupling in GMC, the resulting overall anisotropic response of the composite can be at most orthotropic. In the new model on the other hand there is no such a limitation, and even kidney-shaped inclusions (for example) can be accurately analyzed.

In the present paper, which deals with finite thermoelastic deformation of composites, the derivation of the new micromechanical model is based on a tangential formulation. This formulation establishes the instantaneous concentration tensors (that relate the local deformation gradients and temperature to the global deformation gradients) and the current effective (overall) tangent tensor (that relates the average stress and deformation rates). The derived theory has been applied to a nylon/rubber-like matrix composite under various circumstances. These include thermal loading in which the thermal field is decoupled from the mechanical deformation (one-way coupling), a case that exhibits the thermoelastic inversion effect. In addition, various types of mechanical loading have been investigated such as hydrostatic, axial, transverse and biaxial, all of which illustrate the effect of full thermomechanical coupling on the nonlinear response and the induced average temperature in the composite. It has been shown that the thermomechanical coupling has a strong effect on the nonlinear stress–stretch response of both the monolithic matrix and the composite. For a composite with linearly elastic phases, on the other hand, the effect of coupling on the stress–strain response was much weaker (Williams and Aboudi, 1999).

Acknowledgements

The author gratefully acknowledges the support of the Diane and Arthur Belfer chair of Mechanics and Biomechanics.

Appendix A

In this appendix constitutive relations of a thermoelastic rubber-like material that describe the response of the monolithic rubber phase is established together with the associated coupled energy equation.

A.1. Helmholtz free energy function

The internal energy U per unit mass of a thermoelastic material described as having "modified entropic elasticity" (for a discussion of "entropic elasticity" and "energetic elasticity" see the recent book by Holzapfel, 2000) is represented as the sum of functions of the deformation gradient $\mathbf{F}$ and temperature θ (Chadwick and Creasy, 1984)

$$U(\mathbf{F},\theta) = U_1(\mathbf{F}) + U_2(\theta) \tag{A.1}$$

The Helmholtz free energy per unit mass ψ is given by the standard relation

$$\psi(\mathbf{F},\theta) = U - \theta\eta \tag{A.2}$$

where η is the entropy.

The specific heat at constant deformation is given by

$$c_v = \frac{\partial U}{\partial \theta} \tag{A.3a}$$

It follows from Eq. (A.2) that

$$c_v = \frac{\partial U_2}{\partial \theta} = \theta \frac{\partial \eta}{\partial \theta} \tag{A.3b}$$

where the relation

$$\eta = -\frac{\partial \psi}{\partial \theta} \tag{A.4}$$

has been used.

By integrating Eq. (A.3b) with respect to θ, it follows that the entropy η is also divisible into two parts

$$\eta(\mathbf{F},\theta) = \eta_1(\mathbf{F}) + \eta_2(\theta) \tag{A.5}$$

and

$$c_v = \theta \frac{\partial \eta_2}{\partial \theta} \tag{A.6}$$

Consequently, the free energy can be represented as follows:

$$\psi(\mathbf{F},\theta) = U_1(\mathbf{F}) - \theta\eta_1(\mathbf{F}) + \psi_2(\theta) \tag{A.7}$$

where

$$\psi_2(\theta) = U_2(\theta) - \theta\eta_2(\theta)$$

Let us rewrite Eq. (A.7) in the following form:

$$\psi(\mathbf{F},\theta) = \psi(\mathbf{F},\theta_0)\frac{\theta}{\theta_0} - U_1(\mathbf{F})\left(\frac{\theta}{\theta_0} - 1\right) + \psi_2(\theta) - \psi_2(\theta_0)\frac{\theta}{\theta_0} \tag{A.8}$$

where θ_0 is a reference temperature.

In terms of the Cauchy–Green deformation tensor $\mathbf{C} = \widehat{\mathbf{F}}\mathbf{F}$ ($\widehat{\mathbf{F}}$ denotes the transpose of $\mathbf{F}$), Eq. (A.8) can be further rewritten as

$$\psi(\mathbf{C},\theta) = \psi(\mathbf{C},\theta_0)\frac{\theta}{\theta_0} - U_1(\mathbf{C})\left(\frac{\theta}{\theta_0} - 1\right) + \psi_2(\theta) - \psi_2(\theta_0)\frac{\theta}{\theta_0} \tag{A.9}$$

As in Chadwick and Creasy (1984) and Morman (1995), the following representations of $\psi(\mathbf{C},\theta_0)$ and $U_1(\mathbf{C})$ are assumed

$$\psi(\mathbf{C},\theta_0) = \frac{\mu}{\rho_0} f(\mathbf{C}) + \frac{\kappa}{\rho_0} g(J) \tag{A.10}$$

$$U_1(\mathbf{C}) = \frac{\gamma\mu}{\rho_0} I(\mathbf{C}) + \frac{\kappa\alpha_0\theta_0}{\rho_0} h(J) \tag{A.11}$$

where μ, κ and ρ_0 are the shear modulus, bulk modulus and material density in the undistorted configuration, respectively, α_0 is the initial volume coefficient of thermal expansion, and γ $(0 \leqslant \gamma \leqslant 1)$ is a non-dimensional scalar. In Eqs. (A.10) and (A.11), $f(\mathbf{C})$, $l(\mathbf{C})$, $g(J)$ and $h(J)$ are functions of the corresponding arguments with $J = \det \mathbf{F}$.

The functions $g(J)$ and $h(J)$ are referred to as volumetric response functions, that must satisfy normalization conditions as follows:

$$g(1) = g'(1) = 0, \qquad g''(1) = 1 \qquad h(1) = 0, \qquad h'(1) = 1 \tag{A.12}$$

where prime denotes a differentiation with respect to the argument.

The distorsional functions $f(\mathbf{C})$ and $l(\mathbf{C})$, which vanish in a purely dilatational deformation, have to satisfy certain normalization conditions. For $f(\mathbf{C})$ these conditions are

$$\left.\frac{\partial^2 f}{\partial C_{ij}\partial C_{kl}}\right|_0 = \begin{cases} \frac{1}{3} & (i=j)=(k=l) \\ -\frac{1}{6} & (i=j)\neq(k=l) \\ \frac{1}{4} & (i\neq j)=(k\neq l) \\ \frac{1}{4} & (i=l)\neq(j=k) \\ 0 & \text{otherwise} \end{cases} \tag{A.13}$$

where the subscript 0 indicates evaluation in the reference configuration. Identical conditions are satisfied by the distorsional function $l(\mathbf{C})$. These conditions are consistent with the normalization conditions that have been expressed by Chadwick and Creasy (1984) in terms of the principal stretches.

Using Eqs. (A.10) and (A.11) in (A.9) yields the free energy function

$$\psi(\mathbf{C},\theta) = \frac{\kappa}{\rho_0}\left[g(J)\frac{\theta}{\theta_0} - \alpha_0 h(J)(\theta-\theta_0)\right] + \frac{\mu}{\rho_0}\left[f(\mathbf{C})\frac{\theta}{\theta_0} - \gamma l(\mathbf{C})\left(\frac{\theta}{\theta_0}-1\right)\right] + \psi_2(\theta) - \psi_2(\theta_0)\frac{\theta}{\theta_0} \tag{A.14}$$

A.2. The stress-deformation relations

The Cauchy stress $\boldsymbol{\sigma}$ is obtained from the free energy function (A.14) by employing the relation

$$\boldsymbol{\sigma} = 2\rho\mathbf{F}\frac{\partial\psi}{\partial\mathbf{C}}\widehat{\mathbf{F}} \tag{A.15}$$

where ρ is the current mass density of the material ($\rho_0 = \rho J$). This yields the expression

$$\boldsymbol{\sigma} = \frac{2\kappa}{J}\mathbf{F}\left[g'(J)\frac{\theta}{\theta_0} - \alpha_0 h'(J)(\theta-\theta_0)\right]\frac{\partial J}{\partial\mathbf{C}}\widehat{\mathbf{F}} + \frac{2\mu}{J}\mathbf{F}\left[f'(\mathbf{C})\frac{\theta}{\theta_0} - \gamma l'(\mathbf{C})\left(\frac{\theta}{\theta_0}-1\right)\right]\widehat{\mathbf{F}} \tag{A.16}$$

By employing the identity (Holzapfel, 2000)

$$\frac{\partial J}{\partial\mathbf{C}} = \frac{J}{2}\mathbf{C}^{-1}$$

we readily obtain the expression

$$\boldsymbol{\sigma} = \kappa\left[g'(J)\frac{\theta}{\theta_0} - \alpha_0 h'(J)(\theta-\theta_0)\right]\mathbf{I} + \frac{2\mu}{J}\mathbf{F}\left[f'(\mathbf{C})\frac{\theta}{\theta_0} - \gamma l'(\mathbf{C})\left(\frac{\theta}{\theta_0}-1\right)\right]\widehat{\mathbf{F}} \tag{A.17}$$

where $\mathbf{I}$ is the unit matrix.

It can be verified that the above expression of the Cauchy stress tensor coincides with that of Chadwick and Creasy (1984), Eq. (47), which is given in the principal directions. To this end, let $\mathbf{a} = (a_1, a_2, a_3)$ de-

notes the principal stretches. It follows that $\mathbf{F} = \mathrm{diag}(a_1, a_2, a_3)$, $\mathbf{C} = \mathrm{diag}(a_1^2, a_2^2, a_3^2)$, $f'(\mathbf{C}) = f'(a_i)/2a_i$, and $l'(\mathbf{C}) = l'(a_i)/2a_i$. Substituting these relations in Eq. (A.17) yields

$$\sigma_i(\mathbf{a}, \theta) = \kappa\left[g'(J)\frac{\theta}{\theta_0} - \alpha_0 h'(J)(\theta - \theta_0)\right] + \frac{\mu}{J}a_i\left[\frac{\partial f(\mathbf{a})}{\partial a_i}\frac{\theta}{\theta_0} - \gamma\frac{\partial l(\mathbf{a})}{\partial a_i}\left(\frac{\theta}{\theta_0} - 1\right)\right]$$

which is the required expression of the principal stresses.

A.3. The energy equation

The energy equation in a thermoelastic material is given in the absence of external sources by

$$\rho_0\theta\frac{\partial\eta}{\partial t} = -\mathrm{div}\,\mathbf{q} \tag{A.18}$$

where t is the time and $\mathbf{q}$ is the heat flux vector.

The expression of the entropy η which is needed in Eq. (A.18) can be established from the free energy function (A.14) by using relation (A.4) yielding

$$\eta = -\frac{\kappa}{\rho_0}\left[\frac{g(J)}{\theta_0} - \alpha_0 h(J)\right] - \frac{\mu}{\rho_0}\left[\frac{f(\mathbf{C})}{\theta_0} - \frac{\gamma l(\mathbf{C})}{\theta_0}\right] - \frac{\partial\psi_2(\theta)}{\partial\theta} + \frac{\psi_2(\theta_0)}{\theta_0} \tag{A.19}$$

The rate of accumulation of elastic energy is given by (e.g. Chadwick and Creasy, 1984)

$$e = \dot{U} - \theta\dot{\eta} \tag{A.20}$$

where dot denotes a time derivative. Due to the decomposition of U and η given by Eqs. (A.1) and (A.7) and the use of Eq. (A.3b) it follows that

$$e = \dot{U}_1 - \theta\dot{\eta}_1 \tag{A.21}$$

so that

$$\dot{U}_2 - \theta\dot{\eta}_2 = 0 \tag{A.22}$$

Evaluation of the derivative of $\psi_2(\theta)$ with respect to θ and using (A.22) yield

$$\frac{\partial\psi_2}{\partial\theta} = -\eta_2$$

Thus Eq. (A.19) provides

$$\eta = -\frac{\kappa}{\rho_0}\left[\frac{g(J)}{\theta_0} - \alpha_0 h(J)\right] - \frac{\mu}{\rho_0}\left[\frac{f(\mathbf{C})}{\theta_0} - \frac{\gamma l(\mathbf{C})}{\theta_0}\right] + \eta_2(\theta) + \frac{\psi_2(\theta_0)}{\theta_0} \tag{A.23}$$

Consequently, with the expression of the specific heat c_v given by (A.6), the energy equation (A.18) can be represented in the form

$$\rho_0 c_v\dot{\theta} - \frac{\theta}{\theta_0}\left\{\kappa[\dot{g}(J) - \alpha_0\theta_0\dot{h}(J)] + \mu[\dot{f}(\mathbf{C}) - \gamma\dot{l}(\mathbf{C})]\right\} = -\mathrm{div}\,\mathbf{q} \tag{A.24}$$

By expressing $\mathbf{C}$ in terms of the components of $\mathbf{F}$ one obtains after some manipulations that the energy equation takes the nonlinear coupled heat equation form

$$\rho_0 c_v\dot{\theta} + B_{ik}\dot{F}_{ki} = -\frac{\partial q_i}{\partial X_i} \tag{A.25}$$

where X_i denote the position of a material point in the undeformed configuration at time $t = 0$, and the components of the second-order tensor $\mathbf{B}$ are given by

$$B_{ik} = -\frac{\theta}{\theta_0}\left\{\kappa\left[\frac{\partial g}{\partial J} - \alpha_0\theta_0\frac{\partial h}{\partial J}\right]JC_{ij}^{-1} + 2\mu\left[\frac{\partial f}{\partial C_{ij}} - \gamma\frac{\partial l}{\partial C_{ij}}\right]\right\}F_{kj} \tag{A.26}$$

where C_{ij}^{-1} denotes the ij components of the inverse of $\mathbf{C}$. The uncoupled heat equation is readily obtained from (A.25) by setting $B_{ik} = 0$ (yielding a one-way coupling).

Finally, in the implementation of the energy equation (A.25) the Fourier law is assumed to hold, namely

$$\mathbf{q} = -\kappa_0 \operatorname{grad}\theta \tag{A.27}$$

where κ_0 is the thermal conductivity of the material.

A.4. Specification of the volumetric and distorsional functions

The volumetric response functions $g(J)$ and $h(J)$ can be determined from the pressure-volume-temperature relation of the thermoelastic material. To this end, consider a purely dilatational loading in which $\sigma_{11} = \sigma_{22} = \sigma_{33} = -P$ where P is the applied pressure. It readily follows from constitutive relation (A.17) that

$$P = \kappa\left[\alpha_0 h'(J)(\theta - \theta_0) - g'(J)\frac{\theta}{\theta_0}\right] \tag{A.28}$$

By fitting this relation with measured data for various types of rubbers, Chadwick (1974) obtained the following functions

$$g(J) = \frac{1}{m}\left[J + \frac{J^{1-m}}{m-1} - \frac{m}{m-1}\right] \quad (m > 1) \tag{A.29}$$

$$h(J) = \frac{1}{n}(J^n - 1) \quad (n > 1) \tag{A.30}$$

Both functions satisfy the normalization conditions (A.12).

The distorsional functions $f(\mathbf{C})$ and $l(\mathbf{C})$ were chosen by Morman (1995) as follows:

$$f(\mathbf{C}) = \frac{1}{\mu}\Big[c_{10}\big(I_1 - 3J^{2/3}\big) + c_{01}\big(I_2 - 3J^{4/3}\big) + c_{11}\big(I_1 - 3J^{2/3}\big)\big(I_2 - 3J^{4/3}\big) + c_{20}\big(I_1 - 3J^{2/3}\big)^2 + c_{30}\big(I_1 - 3J^{2/3}\big)^3\Big] \tag{A.31}$$

where c_{10}, c_{01}, c_{11}, c_{20}, c_{30} are material constants, and I_1 and I_2 are the first and second invariants of $\mathbf{C}$, namely,

$$I_1 = \operatorname{tr}\mathbf{C} = C_{ii}$$

$$I_2 = \frac{1}{2}\big(\operatorname{tr}^2\mathbf{C} - \operatorname{tr}\mathbf{C}^2\big)$$

and

$$l(\mathbf{C}) = (1-\gamma)f(\mathbf{C}) \tag{A.32}$$

It should be noted that under dilatational loading in which $F_{11} = F_{22} = F_{33}$ it can be readily verified that $f(\mathbf{C})$ vanishes, as well as the derivatives of $f(\mathbf{C})$ with respect to $\mathbf{C}$.

A.5. Tangential formulation

The micromechanical analysis that is presented in this paper is based on a tangential formulation that is formulated in terms of the first Piola–Kirchhoff stress tensor (which represents the actual stresses). Consequently, Eq. (A.17) that expresses the constitutive equation of the rubber-like phase, must be reformulated such that the rate of the first Piola–Kirchhoff stress tensor $\dot{\mathbf{T}}$ is expressed in terms of the rate of the deformation gradient $\dot{\mathbf{F}}$ and the rate of temperature $\dot{\theta}$. The utilization of a tangential formulation in the micromechanical incremental procedure has the advantage that it prevents the need to solve a system of nonlinear algebraic equations at each increment. Instead, a linear system needs to be solved which is a significant advantage. To this end, let us express the first Piola–Kirchhoff stress tensor $\mathbf{T}$ in terms of Cauchy stress tensor $\boldsymbol{\sigma}$ (Malvern, 1969):

$$\mathbf{T} = J\mathbf{F}^{-1}\boldsymbol{\sigma} \tag{A.33}$$

The required tangential form of the nonlinear thermomechanical constitutive relation is given by

$$\dot{\mathbf{T}} = \mathbf{R}\dot{\mathbf{F}} - \mathbf{H}\dot{\theta} \tag{A.34}$$

The fourth order tensor $\mathbf{R}$ is the instantaneous mechanical tangent tensor, while the second order tensor $\mathbf{H}$ represents the instantaneous thermal tangent tensor. These tangent tensors are obtained from the derivatives $\partial T_{ij}/\partial F_{kl}$ and $-\partial T_{ij}/\partial\theta$, respectively. In evaluating these derivatives, one needs to differentiate $\boldsymbol{\sigma}$ with respect to the deformation gradient components F_{kl} as well as with respect to the temperature θ. In addition, the derivatives of J and $\mathbf{F}^{-1}$ with respect to $\mathbf{F}$ are also needed. All expressions needed in evaluating these derivatives are presented in Appendix B.

Appendix B

In this appendix all the derivatives needed in the evaluation of the mechanical tangent tensor $R_{ijkl} = \partial T_{ij}/\partial F_{kl}$, and the thermal tangent stress tensor $H_{ij} = -\partial T_{ij}/\partial\theta$ are given below:

$$\frac{\partial C_{ij}}{\partial F_{pq}} = \delta_{iq}F_{pj} + \delta_{jq}F_{pi}$$

where δ_{ij} is the Kronecker delta. Furthermore,

$$\left.\begin{aligned} \tfrac{\partial I_1}{\partial C_{ij}} &= \delta_{ij} \\ \tfrac{\partial I_2}{\partial C_{ij}} &= I_1\delta_{ij} - C_{ij} \\ \tfrac{\partial I_3}{\partial C_{ij}} &= I_2\delta_{ij} - I_1C_{ij} + C_{ik}C_{kj} \end{aligned}\right\}$$

and

$$\frac{\partial^2 I_1}{\partial C_{ij}\partial C_{kl}} = 0$$

$$\frac{\partial^2 I_2}{\partial C_{ij}\partial C_{kl}} = \delta_{ij}\delta_{kl} - I^{(4)}_{ijkl}$$

$$\frac{\partial^2 I_3}{\partial C_{ij}\partial C_{kl}} = (I_1\delta_{kl} - C_{kl})\delta_{ij} - C_{ij}\delta_{kl} - I_1I^{(4)}_{ijkl} + \frac{1}{2}\left(\delta_{ik}C_{jl} + \delta_{il}C_{jk}\right) + \frac{1}{2}\left(C_{ik}\delta_{jl} + C_{il}\delta_{jk}\right)$$

where

$$I^{(4)}_{ijkl} = \tfrac{1}{2}(\delta_{ik}\delta_{jl} + \delta_{il}\delta_{jk})$$

In addition

$$\frac{\partial F^{-1}_{ij}}{\partial F_{pq}} = -F^{-1}_{ip}F^{-1}_{qj}$$

$$\frac{\partial J}{\partial F_{ij}} = JC^{-1}_{jp}F_{ip}$$

where F^{-1}_{ij} and C^{-1}_{ij} denote the ij components of the inverse of the deformation gradient **F** and the Cauchy–Green deformation tensor **C**, respectively.

Finally, $\partial J/\partial C_{ij} = JC^{-1}_{ij}/2$ as has been already given in the text, and

$$\frac{\partial^2 J}{\partial C_{ij}\partial C_{kl}} = \frac{J}{4}\left[C^{-1}_{ij}C^{-1}_{kl} - 2C^{-1}_{ik}C^{-1}_{jl}\right]$$

References

Aboudi, J., 1996. Micromechanical analysis of composites by the method of cells-update. Appl. Mech. Rev. 49, S83–S91.

Aboudi, J., 2001a. Micromechanical prediction of the finite thermoelastic response of rubber-like matrix composites. J. Appl. Mech. Phys. (ZAMP) 52, 823–846.

Aboudi, J., 2001b. Micromechanical analysis of fully coupled electro-magneto-thermo-elastic multiphase composites. Smart Mater. Struct. 10, 867–877.

Aboudi, J., Pindera, M-J., Arnold, S.M., 1999. Higher-order theory for functionally graded materials. Compos.: Part B (Eng.) 30, 777–832.

Aboudi, J., Pindera, M-J., Arnold, S.M., 2001. Linear thermoelastic higher-order theory for periodic multiphase materials. J. Appl. Mech. 68, 697–707.

Aboudi, J., Pindera, M-J., Arnold, S.M., 2002. Higher-order theory for periodic multiphase materials with inelastic phases. Int. J. Plasticity.

Agah-Tehrani, A., 1990. On finite deformation of composites with periodic microstructure. Mech. Mater. 8, 255–268.

Banks-Sills, L., Leiderman, V., Fang, D., 1997. On the effect of particle shape and orientation on elastic properties of metal matrix composites. Compos. Part B 28B, 465–481.

Chadwick, P., 1974. Thermo-mechanics of rubber-like materials. Phil. Trans. Royal Soc. London A 276, 372–403.

Chadwick, P., Creasy, C.F.M., 1984. Modified entropic elasticity of rubber-like material. J. Mech. Phys. Solids 5, 337–357.

Holzapfel, G.A., 2000. Nonlinear Solid Mechanics. John Wiley, New York.

Jansson, S., 1992. Homogenized Nonlinear constitutive properties and local stress concentrations for composites with periodic internal structure. Int. J. Solids Struct. 29, 2181–2200.

Li, J.Y., Dunn, M.L., 1998. Micromechanics of magnetoelectroelastic composite materials: average field and effective behavior. J. Intell. Mater. Syst. Struct. 9, 404–416.

Malvern, L.E., 1969. Introduction to the Mechanics of Continuous Medium. Prentice Hall, Englewood Cliffs, New Jersey.

Mori, T., Tanaka, K., 1973. Average stresses in matrix and average energy of materials with misfitting inclusions. Acta Metall. 21, 571–574.

Morman, K.N., 1995. A thermomechanical model for amorphous polymers in the glassy, transition, and rubber regions. In: Current Research in the Thermo-Mechanics of Polymers in the Rubbery-Glassy Range, AMD-vol. 203. ASME, New York.

Ogden, R.W., 1992. On the thermoelastic modeling of rubber-like solids. J. Thermal Stresses 15, 533–557.

Perry, J.H., 1963. Chemical Engineers' Handbook. McGraw-Hill, New York.

Price, C., 1976. Thermodynamics of rubber elasticity. Proc. Royal Soc. London A 351, 331–350.

Suquet, P.M., 1987. Elements of homogenization for inelastic solid mechanics. Lecture Notes Phys. 272, 193–278.

Takano, N., Ohnishi, Y., Zako, M., Nishiyabu, K., 2000. The formulation of homogenized method applied to large deformation problem for composite materials. Int. J. Solids Struct. 37, 6517–6535.

Treloar, L.R.G., 1975. The Physics of Rubber Elasticity. Oxford University Press, Oxford.

Williams, T.O., Aboudi, J., 1999. A fully coupled thermomechanical micromechanics model. J. Thermal Stresses 22, 841–873.